

# Winding Numbers and Topology of Aperiodic Tilings

Yaroslav Don and Eric Akkermans\*

*Department of Physics, Technion – Israel Institute of Technology, Haifa 3200003, Israel*

(Dated: October 19, 2021)

We show that diffraction features of  $1D$  quasicrystals can be retrieved from a single topological quantity, the Čech cohomology group,  $\check{H}^1 \cong \mathbb{Z}^2$ , which encodes all relevant combinatorial information of tilings. We present a constructive way to calculate  $\check{H}^1$  for a large variety of aperiodic tilings. By means of two winding numbers, we compare the diffraction features contained in  $\check{H}^1$  to the gap labeling theorem, another topological tool used to label spectral gaps in the integrated density of states. In the light of this topological description, we discuss similarities and differences between families of aperiodic tilings, and the resilience of topological features against perturbations.

Aperiodic tilings are structures obtained from the spatial arrangement of motives according to a set of deterministic rules [1, 2]. They constitute a rich playground to investigate a wealth of new ideas and features of physical systems in different contexts, such as condensed matter, statistical mechanics, dynamical systems and new materials. This ubiquity is partly due to the existence of a large set of tiling families including periodic, nonperiodic (e.g. Wang tiles), quasiperiodic, and asymptotically periodic tilings.

A celebrated family of aperiodic tilings are quasicrystals [3, 4]. Despite their lack of periodicity, they exhibit Bragg peaks. Spectral characteristics of propagating waves (acoustic, optical, matter) in quasicrystals reveal a highly lacunar fractal energy spectrum, with an infinite set of energy gaps [5–8]. The gap labeling theorem (GLT) [9, 10] provides a framework for the description of these gaps. Where Bloch theorem allows to label energy eigenstates with a quasi-momentum and to identify topological numbers expressed in terms of a Berry curvature [11–14], the GLT assigns a set of integers to each gap in the spectrum of aperiodic tilings. These integers can be given a topological meaning akin in nature to Chern numbers or alike, but different in many respects and not expressible in terms of a curvature [9, 15]. Topological features of aperiodic tilings are still largely uncharted despite extensive interest, and situations where they can be directly measured in an experiment remain an exception [16–21]. A reason for this state of affairs is that topological features of tilings are often established in the limit of infinite systems, whereas finite size measurable aperiodic samples cannot be unequivocally discriminated from periodic tilings of appropriate unit cells. As a consequence, topological properties of aperiodic tilings are often dimmed and considered irrelevant [22–24].

Our purpose is to present a systematic and easily implemented description of topological aspects of aperiodic tilings in terms of (integer) winding numbers of two phases respectively associated to structural and spectral features. This description holds for finite size tilings in any dimension. For quasicrystals, these two phases are equivalent, thus leading to an extension of Bloch theorem beyond periodic systems [25]. For other aperiodic

tilings, this equivalence does not hold. Finally, our approach offers a simple description of GLT and related topological aspects which, despite their importance, are often difficult to decipher. In addition, it will help unifying disparate accounts of structural and spectral properties of tilings scattered in different parts of an abundant literature on that subject.

To convey essential ideas of our description and to define the two phases and their winding numbers, we first consider  $1D$  tilings built out of a two-letter  $\{A, B\}$  alphabet, each representing a tile of respective length  $\{l_A, l_B\}$  with an atom inserted on the boundary between adjacent tiles. The atomic density is  $\rho(x) = \sum_i \delta(x - x_i)$ , where  $x_i = \sum_{j=1}^i l_j$  is the atom location. The Fourier transform  $\hat{\rho}(k)$  of  $\rho$  is a complex valued function whose modulus determines the structure factor  $S(k) = |\hat{\rho}(k)|^2$  of the tiling namely its diffraction spectrum. We denote  $\Theta_d(k) = \arg \hat{\rho}(k)$  the phase of  $\hat{\rho}(k)$ . It is the first relevant phase we consider and it accounts for structural data of tilings.

The band structure of excitations (e.g. electronic, electromagnetic, acoustic or mechanical waves) propagating in a tiling is modeled either by a tight-binding model with particles hopping from tile to tile or by a continuous wave equation (e.g. Schrödinger or Helmholtz). The quantum/wave mechanical description involves a certain self-adjoint operator in the space of square-summable functions in the set of tiles. We are interested in its energy/frequency spectrum, a well documented problem in condensed matter literature [26]. The counting function  $\mathcal{N}(E)$ , or integrated density of states (IDOS), is the fraction of eigenenergies smaller than a given value  $E$ . For large enough system size,  $\mathcal{N}(E)$  is independent of the choice of boundary conditions and it is a well defined and continuous function of energy. A convenient description of spectral properties is provided by the scattering matrix formalism where, in  $1D$ , a  $2 \times 2$  unitary operator  $\mathcal{S}(E)$  maps ingoing onto outgoing waves scattered by a finite size tiling. Diagonalising  $\mathcal{S}(E)$  leads to two independent phases: the scattering phase shift  $\delta(E) = \text{Im} \log \det \mathcal{S}(E)$ , allows to determine the counting function,  $\mathcal{N}(E) = \delta(E)/\pi$  [26] (see Supplementary Material (SM) [27, Sec. D2]); and the chiral

phase [28, 29],

$$\Theta_s(E) = \text{Im Tr} [\sigma_z \log \mathcal{S}(E)], \quad (1)$$

where  $\sigma_z = \text{diag}(1 \ -1)$  is the Pauli matrix, displays topological features. To unveil them, we consider the (integer) winding numbers  $\mathcal{W}_\phi[\Theta_d]$  and  $\mathcal{W}_\phi[\Theta_s]$  w.r.t. an angular variable  $\phi$  (defined below) of the two phases  $\Theta_d$  and  $\Theta_s$  and show that they result from the existence of a topological invariant of the tiling, its Čech cohomology group  $\check{H}^1$ , a quantity we define and compute systematically. To that purpose, we start with the case of 1D quasicrystals. Rediscovering well established results using a new approach should not hinder that it is applicable far more generally as we shall see.

A quasicrystal in dimension  $D$  is modeled as a section of a periodic lattice (crystal) in a  $n$ -dimensional superspace  $\mathbb{R}^n$ , with  $n > D$ . We have the decomposition  $\mathbb{R}^n = E^\parallel \oplus E^\perp$ , where  $E^\parallel$  is the  $D$ -dimensional physical space in which the structure is embedded, whereas  $E^\perp$  is an  $(n - D)$ -dimensional internal space. This setting is implemented for the Cut & Project algorithm (hereafter, C&P) [1, 30–32]. For a 1D-quasiperiodic tiling, the superspace is the square lattice  $\mathbb{Z}^2$  and the physical space is the line  $E^\parallel$  making a tilt angle  $\theta$  with the horizontal axis. An irrational slope  $s = 1/(1 + \cot \theta)$  leads to a quasiperiodic tiling, while an irreducible rational  $s = p/q$ , corresponds to a periodic structure with  $q$  atoms in a cell. A celebrated example is the Fibonacci quasicrystal obtained for the irrational slope  $s = \tau^{-1} = 2/(1 + \sqrt{5})$ . The location of the cut-line in the  $E^\perp$  direction (see SM [27, Sec. A1]) is an additional degree of freedom  $\phi \in [0, 2\pi]$  called phason.

To describe finite size tilings, it is convenient to expand the slope  $s$  as a continued fraction  $c_N/d_N \xrightarrow{N \rightarrow \infty} s$  (see SM [27, Sec. A2]) so that the phason becomes discrete,  $\phi \mapsto \phi_\ell = 2\pi\ell/d_N$  with  $\ell = 0 \dots d_N - 1$ . The number of distinct words, i.e. of finite tilings, of size  $L$  is  $L + 1$  [33, 34], and for the  $N$ -th approximation ( $L = d_N$ ), there are  $d_N$  words, which are mutual cyclic permutations [35]. Consider a representative word  $w_0$  from the mutually-cyclic ones, and define the  $d_N \times d_N$  characteristic matrix

$$\Sigma_1(n, \ell) = \mathcal{T}^{m(\ell)}[w_0(n)], \quad (2)$$

with  $m(\ell) = \ell c_N^{-1} \pmod{d_N}$ , and  $\mathcal{T}[w_0(n)] = w_0(n + 1)$  the translation operator with periodic boundary conditions in both  $n$  and  $\ell$  directions. Thus, all the rows of  $\Sigma_1$  are cyclic permutations of each other. Hence,  $\Sigma_1$  is a torus (see Fig. 1), whose discrete Fourier transform about  $n$  is

$$G_N(\xi, \ell) = \sum_{n=0}^{d_N-1} \omega^{-\xi n} \Sigma_1(n, \ell) = \omega^{m(\ell)\xi} \varsigma_0(\xi), \quad (3)$$

where  $\omega = \exp(2\pi i/d_N)$ , and  $\varsigma_0(\xi)$  is the Fourier transform of  $w_0(n)$ . The structure factor  $S_N(\xi, \phi) =$

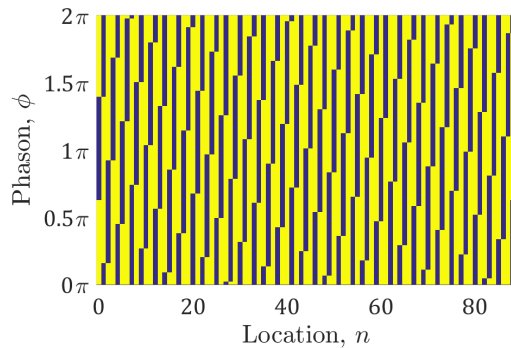


Figure 1. The characteristic function  $\Sigma_1$  for the Fibonacci sequence with  $d_N = 89$ . The  $A$  ( $B$ ) tiles with  $\Sigma_1 = +1$  ( $-1$ ) are drawn in yellow (blue). Each row represents a word of length  $d_N$ .

$|\varsigma_0(\xi)|^2/d_N$  is  $\phi$ -independent. However, the *structural* phase  $\Theta_d(\xi, \ell) = \arg G_N(\xi, \ell)$  reads

$$\Theta_d(\xi, \ell) = \phi_\ell \xi / c_N + \alpha_0(\xi) \pmod{2\pi}. \quad (4)$$

where  $\alpha_0(\xi) = \arg \varsigma_0(\xi)$  is  $\phi$ -independent. Thus, for any diffraction (discrete Bragg) peak  $\xi_{p,q} = qc_N$ , the winding number is  $\mathcal{W}_\phi[\Theta_d(\xi_{p,q}, \phi)] = q$ , as displayed in Fig. 2a.

We now consider spectral features of tilings encoded in the  $\phi$ -dependent scattering matrix  $\mathcal{S}(E, \phi)$  and the phase  $\Theta_s(E, \phi)$  from (1). Its winding inside a gap is  $\mathcal{W}_\phi[\Theta_s(E_g, \phi)] = 2q$  [20], as displayed numerically in Fig. 2b. The winding numbers of the two phases, structural and spectral, thus fulfill [35]

$$2\mathcal{W}_\phi[\Theta_d] = \mathcal{W}_\phi[\Theta_s] = 2q. \quad (5)$$

The integer  $q$  also appears in the structure factor and the counting function  $\mathcal{N}(E_g)$  in the gaps [10], since both the positions  $k_b/k_0$  of the normalized and infinite countable set of Bragg peaks [1] and the gap locations in the energy spectrum are related to the irrational slope  $s$  by

$$k_b/k_0 = p + qs = \mathcal{N}(E_g), \quad p, q \in \mathbb{Z}. \quad (6)$$

This one-to-one correspondence between Bragg peaks and spectral gap locations is not coincidental, it rather reflects the equivalence between structural and spectral data of C&P quasiperiodic 1D tilings. The meaning of  $q$  as a common winding number in (5) constitutes one important result of this letter and an obvious appeal to topology.

Note that (5) does not yet provide a clear connection to topological quantities nor a systematic procedure to calculate them akin to Chern numbers and Berry curvature for periodic structures. Results similar to (5) have been obtained for 1D continuous wave equations in a quasiperiodic potential [36, 37], and for tight-binding operators [38] and have been subsequently extended to more general tilings by Bellissard [9] and Luck [5]. A topological

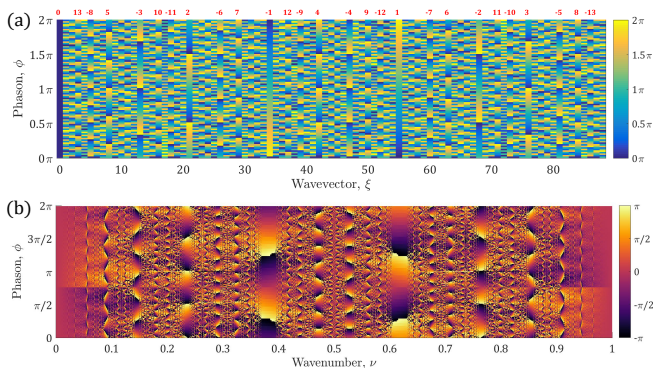


Figure 2. Topological phases of the Fibonacci tiling with slope  $s = (\sqrt{5} - 1)/2$ . (a) The structural phase  $\Theta_d(\xi, \phi)$  with  $d_N = 89$  sites. Windings are indicated by the red numbers above. (b) The chiral phase  $\Theta_s(\nu, \phi)$  with  $d_N = 233$  sites using  $(n_A, n_B) = (1, 1.15)$  and  $(l_A, l_B) = (1.15, 1)$ . The wavenumber  $\nu$  is the normalized wavevector  $k$ .

interpretation of the gap labeling as a winding number has been underlined. Yet, that interpretation used the rotation number, which is essentially equivalent to the total phase shift  $\delta(E)$  – a quantity that is distinct from the winding of  $\Theta_s$  w.r.t. the phason  $\phi$ .

We now show that both diffraction and spectral features are fully characterised by a topological invariant systematically computable and directly related to the winding numbers in (5). To illustrate these ideas, we introduce the notion of substitution to generate structural data of 1D C&P aperiodic tilings [1, 30, 39, 40].

For a two-letter alphabet  $\{A, B\}$ , a substitution rule is defined by its action  $\sigma$  on a word  $w = l_1 l_2 \dots l_k$ , where  $l_i = A$  or  $B$ , by the concatenation  $\sigma(w) = \sigma(l_1) \sigma(l_2) \dots \sigma(l_k)$ . A primitive occurrence matrix,  $M = \begin{pmatrix} \alpha & \beta \\ \gamma & \delta \end{pmatrix}$  defined by  $\sigma(A) = A^\alpha B^\beta$  and  $\sigma(B) = A^\gamma B^\delta$ , is associated to  $\sigma$ . Its largest eigenvalue  $\lambda_*$  is larger than 1 (Frobenius-Perron theorem). Its left eigenvector  $\mathbf{v}_* = (\varrho_A, \varrho_B)$  coincides with the corresponding letter densities in the infinite tiling. For the Fibonacci substitution,  $M = \begin{pmatrix} 1 & 1 \\ 0 & 1 \end{pmatrix}$ ,  $\lambda_* = \tau = \frac{1+\sqrt{5}}{2}$ ,  $(\varrho_A, \varrho_B) = (\tau^{-1}, \tau^{-2})$ . The C&P and substitution algorithms are not equivalent, e.g. no substitution is associated to the C&P slope  $s = 1/\pi$  since  $\pi$  is a transcendental and not an algebraic irrational. Inversely, the substitution  $M = \begin{pmatrix} 1 & 2 \\ 0 & 1 \end{pmatrix}$  has no C&P counterpart. But if  $\lambda_*$  is an algebraic rational, it may correspond to a C&P tiling of slope  $s = \varrho_B$ , a situation that we now consider.

Denote  $w_\infty$  the infinite tiling/word and consider all  $n$ -letter words (also known as supertiles)  $\Gamma_n = \{w \in w_\infty : |w| = n\}$ . Next, define the shift  $\gamma_n : \Gamma_n \rightarrow \Gamma_n$  by  $\gamma_n(w_i) = w_j$  if  $w_j$  follows  $w_i$  in  $w_\infty$ . We define Bratteli diagrams by  $G_n = (\Gamma_n, \gamma_n)$ . For example, for the Fibonacci tiling,

$$\Gamma_1^{\text{Fib}} = \{A, B\} \quad (7a)$$

$$\Gamma_2^{\text{Fib}} = \{AA, AB, BA\} \quad (7b)$$

$$\Gamma_3^{\text{Fib}} = \{AAB, ABA, BAA, BAB\} \quad (7c)$$

so that

$$G_1^{\text{Fib}} = AA \begin{array}{c} \circlearrowleft \\ \circlearrowright \end{array} \begin{array}{c} A \\ B \end{array} \begin{array}{c} \circlearrowright \\ \circlearrowleft \end{array} \quad (8a)$$

$$G_2^{\text{Fib}} = \begin{array}{c} AAB \\ \circlearrowleft \\ AA \\ \circlearrowright \\ BAA \end{array} \begin{array}{c} AB \\ BA \end{array} \begin{array}{c} \circlearrowright \\ \circlearrowleft \end{array} \quad (8b)$$

Each node of  $G_n$  is a supertile element of  $\Gamma_n$ , and each edge is a supertile element of  $\Gamma_{n+1}$ , so that at each level  $n$ , the (oriented) Bratteli graph  $G_n$  indicates how successive supertiles are encountered while moving along the infinite tiling  $w_\infty$ .

We are interested in the number  $\beta_n$  of independent closed cycles of the oriented graph  $G_n$ , i.e. in the number of independent ways to move along the tiling either finite or infinite. It is clear that  $\beta_1 = \beta_2 = 2$ . For instance, using  $\Gamma_1$  tiles, the graph  $G_1$  shows that it exists two independent ways to move along a Fibonacci tiling, so that any finite length sequence can be decomposed into a linear combination of two closed cycles:  $A \rightarrow A$  and  $A \rightarrow B \rightarrow A$ . Should we decide to explore the tiling using supertiles  $\Gamma_2$ , then again any evolution along the tiling involves a linear combination of two closed cycles:  $AB \rightarrow BA \rightarrow AB$  and  $AA \rightarrow AB \rightarrow BA \rightarrow AA$ . This decomposition into linear combination of independent closed cycles of supertiles  $\Gamma_n$  with integer coefficients has a group structure isomorphic to  $\mathbb{Z}^{\beta_n}$ , known as the cohomology  $H^n(G_n, \mathbb{Z})$  (see SM [27, Sec. C1]). The limiting process  $n \rightarrow \infty$ , if it exists, defines the Čech cohomology group  $\check{H}^1$ , a topological invariant of the tiling. For 1D C&P quasicrystals,  $\beta_n = 2$  for all  $n$  (see SM [27, Sec. C3]), namely the evolution along any sequence involves a linear combination of two cycles independently of the chosen supertile.

To systematically compute  $\check{H}^1$  for aperiodic tilings, the knowledge of the application of the inflation rule on Bratteli diagrams is needed. Consider a substitution  $\sigma$  and the Bratteli diagram  $G_2$  as in (8). Next, apply  $\sigma$  on  $G_2$  to generate the diagram (for the Fibonacci case)

$$\sigma(G_2^{\text{Fib}}) = \begin{array}{c} \begin{array}{c} ABA \\ \circlearrowleft \\ AB \\ \circlearrowright \\ BA \end{array} \begin{array}{c} AB \\ BA \end{array} \begin{array}{c} \circlearrowright \\ \circlearrowleft \end{array} \\ \begin{array}{c} BAB \\ \circlearrowleft \\ AB \\ \circlearrowright \\ AAB \end{array} \begin{array}{c} BA \\ AA \end{array} \begin{array}{c} \circlearrowright \\ \circlearrowleft \end{array} \end{array} \quad (9)$$

Identifying the nodes and edges between  $G_2^{\text{Fib}}$  and  $\sigma(G_2^{\text{Fib}})$  (see SM [27, Sec. C2]), we infer the inflation matrices

$$A_1^\Gamma = \begin{pmatrix} 0 & 1 & 0 & 1 \\ 0 & 1 & 1 & 0 \\ 1 & 0 & 0 & 0 \\ 1 & 0 & 0 & 0 \end{pmatrix}, \quad A_0^\Gamma = \begin{pmatrix} 0 & 1 & 0 \\ 0 & 1 & 0 \\ 1 & 0 & 0 \end{pmatrix}. \quad (10)$$

Defining the  $\zeta$ -function [41],

$$\zeta(z) = \frac{\det(I - zA_0^T)}{\det(I - zA_1^T)} = \frac{p_0(z)}{p_1(z)}, \quad (11)$$

the Čech cohomology is then retrieved from the decomposition of the polynomials  $p_0(z)$  and  $p_1(z)$  into their irreducible components over the integers, and given by the direct sum of  $\mathbb{Z}$  adjoined by their leading coefficients (see SM [27, Sec. C2]). For Fibonacci,  $p_0(z) = 1 - z$  and  $p_1(z) = 1 - z - z^2$  inferring  $\check{H}^1 \cong \mathbb{Z}^2$ —independently of the irrational slope  $s$ . In C&P quasicrystals,  $\check{H}^1$  corresponds to the incongruent dimensions of  $\mathbb{R}^n$  with respect to  $E^\parallel$ . In 1D tilings originated in  $\mathbb{R}^2$ ,  $\check{H}^1 \cong \mathbb{Z}^2$  if  $s$  is irrational, and  $\check{H}^1 \cong \mathbb{Z}$  if  $s \in \mathbb{Q}$ .

We now show that winding numbers  $\mathcal{W}_\phi[\Theta_d]$  in (5) and Bragg peaks at locations (6), are direct consequences of the topological property,  $\check{H}^1 \cong \mathbb{Z}^2$ .

For irrational slopes  $s$ , there are 2 cycles, which for each  $N$  and  $s_N = c_N/d_N$  approximant, consist of a long  $d_N$ -cycle made of  $d_N$  cyclically permuted  $d_N$ -supertiles and a short cycle of length  $d_{N-1}$ . Since the approximant  $s_N$  is rational, only the long cycle remains for  $n \geq d_N - 1$ . Cyclically permuting a given supertile  $t_N$  (of length  $d_N$ ) by  $c_N^{-1} \pmod{d_N}$  tiles results in the same supertile up to a single pair switch (see Fig. 1). This is the winding property expressed in (4) and (5).

To show the existence and locations of Bragg peaks, consider for each  $N$  and  $s_N = c_N/d_N$  approximant, the structure factor  $S_N(\xi) = |G_N(\xi)|^2/d_N$  where  $\xi = kd_N$  and  $G_N(\xi)$  is the discrete Fourier transform (3) of supertiles  $t_N$  of length  $d_N$ . It has positive contributions for each  $\xi_l = l + d_N p$ , thus producing diffraction peaks at  $S_N(\xi) = \sum_{p \in \mathbb{Z}} \sum_{l=0}^{d_N-1} a_l \delta_{\xi, l+d_N p}$ . Furthermore, using the winding property above, the diffraction of *permuted* supertiles reads,  $\tilde{S}_N(\xi) \simeq d_N^{-1} e^{2\pi i c_N^{-1} \xi} |G_N(\xi)|^2 = e^{2\pi i c_N^{-1} \xi} S_N(\xi)$ . Since  $S_N$  and  $\tilde{S}_N$  must match, then  $e^{2\pi i c_N^{-1} \xi} = 1$  implying  $\xi_q = c_N q$ . Hence,

$$S_N(\xi) = \sum_{p \in \mathbb{Z}} \sum_{q=0}^{d_N-1} a_q \delta_{\xi, c_N q + d_N p}. \quad (12)$$

Overall, there are two copies of  $S_N(k)$  at each order  $N$ . Changing to  $k = \xi/d_N$  in (12) and taking the limit  $N \rightarrow \infty$  gives [35]

$$S(k) = \sum_{p \in \mathbb{Z}} \sum_{q \in \mathbb{Z}} \bar{a}_q \delta(k - (p + sq)), \quad (13)$$

as announced in (6).

We have thus proven that for 1D C&P tilings, the topological invariant  $\check{H}^1 \cong \mathbb{Z}^2$  and the associated winding numbers (5), provide the set of integers needed to describe the structure factor (13). These results have been summarized [25] using a trace map, denoted  $\tau_*^d(\check{H}^1)$

between  $\check{H}^1 \cong \mathbb{Z}^2$  and the group  $\mathbb{Z} + s\mathbb{Z}$ , namely  $\tau_*^d(\check{H}^1 \cong \mathbb{Z}^2) = \mathbb{Z} + s\mathbb{Z}$ .

The excitation spectrum and gap locations of operators defined on 1D C&P tilings are also characterised by two integers (6), a result quantified in the GLT [9]. Winding numbers  $\mathcal{W}_\phi[\Theta_s]$  in (5) at these gaps, are also consequences of topological features of the tiling. As proven in [9] using the  $K_0$  group, gap locations are obtained from another trace map here denoted  $\tau_*^s(K_0)$ . In [25], the equivalence of these two traces has been established for 1D C&P quasiperiodic tilings, namely  $\tau_*^d(\check{H}^1) = \tau_*^s(K_0) = \mathbb{Z} + s\mathbb{Z}$ , a result essentially expressed by (6).

However, as appealing as it may seem, this equivalence between diffraction and spectral features does not apply to all aperiodic tilings. The reason for that is to be found in the physical contents of the Čech cohomology group  $\check{H}^1$  and the GLT. A main feature behind the GLT—sometimes hidden by the non trivial mathematics—is that the possible values  $\mathcal{N}$  of the IDOS on the gaps are given by the densities  $\varrho_w$  of all possible words  $w$  in the infinite tiling, viz.  $\mathcal{N}_w = \varrho_w$ . Stated otherwise, for a gap to open in the IDOS, it is necessary that some word appears infinitely many times (a condition also shared by periodic tilings). For the two-letter  $\{A, B\}$  alphabet,  $A$  and  $B$  tiles imply gaps on  $\mathcal{N} = \varrho_A$  and  $\mathcal{N} = \varrho_B$ . To find the other densities for substitution tilings (see SM [27, Sec. B]), one requires an updated rule  $\sigma_n : \Gamma_n \rightarrow \Gamma_n$  with its occurrence matrix  $M_n$  for each  $n$ . For primitive substitutions, the leading eigenvalue  $\lambda_*$  is the same for all  $M_n$ , and the densities are given by the leading eigenvector  $\mathbf{v}_{*,n}$ . The eigenvectors  $\mathbf{v}_*$  and  $\mathbf{v}_{*,2}$  together with  $\lambda_*$  suffice to span all other densities [42]. Thus, the GLT [9] allows to compute

$$\mathcal{N}_{k,N}(E_g) = \frac{1}{a} \frac{k}{\lambda_*^N} \pmod{1}, \quad k, N \in \mathbb{N}, \quad (14)$$

where  $a$  is the least common multiplier of all elements of  $\mathbf{v}_*$  and  $\mathbf{v}_{*,2}$  (see SM [27, Sec. B]). For quasiperiodic substitutions which have  $\det(M) = \pm 1$ , (14) reduces to

$$\mathcal{N}_{p,q}(E_g) = a^{-1} (p + q/\lambda_*) \pmod{1}, \quad p, q \in \mathbb{Z}, \quad (15)$$

namely, the densities for  $w_n$  are integral linear combinations of 1 and  $s$  implying (6) and equivalent to  $\tau_*^s(K_0) = \mathbb{Z} + s\mathbb{Z}$ . Therefore, the existence and location of gaps are essentially counting properties of tilings encapsulated in the distribution of word frequencies—a positive measure expressed by the normalised eigenvectors  $\mathbf{v}_*$  and  $\mathbf{v}_{*,2}$ . In contrast, the cohomology group  $\check{H}^1$  includes information on *how to order* the words, i.e. their combinatorial properties; thus its relevance to the diffraction spectrum. But for 1D C&P tilings,  $\check{H}^1$  also accounts for words' densities  $\varrho_w$ , hence the equivalence  $\tau_*^d(\check{H}^1) = \tau_*^s(K_0) = \mathbb{Z} + s\mathbb{Z}$  [25] which generally holds for tilings with Bragg diffraction spectrum.

A remarkable example to sharpen this distinction is the Thue-Morse tiling:  $\sigma_{\text{TM}}(A) = AB$ ,  $\sigma_{\text{TM}}(B) = BA$ . It shares the same occurrence matrix  $M = \begin{pmatrix} 1 & 1 \\ 1 & 1 \end{pmatrix}$  with the periodic substitution  $\sigma_{\text{per}}(A) = \sigma_{\text{per}}(B) = AB$ . Despite this, their structure factor and spectral gap distribution are completely different, a result to be associated to the different orderings of words of all lengths. From (14), the Thue-Morse tiling has a singular continuous distribution of gaps on  $\mathcal{N} = \frac{1}{3} m/2^N$ , but a complex and still unclear singular continuous diffraction component. Experimentally measured in [43], diffraction peaks were announced to be located at  $k/k_0 = \frac{1}{3} m/2^N$ . A different formula  $k/k_0 = \frac{1}{p} m/2^N$  was reported by [5, 44, 45] ( $p$  odd), [46] ( $p$  prime), [47] ( $p = 2^n - 1$ ), and [48] (various  $p$  with positive scaling exponents). On top of that, Thue-Morse admits Bragg diffraction for  $k_b/k_0 = m, m + \frac{1}{2}$  for  $m \in \mathbb{Z}$  [47]. This behaviour is not captured by the GLT formula but it is implied by  $\check{H}_{\text{TM}}^1 \cong \mathbb{Z} \oplus \mathbb{Z}[\frac{1}{2}]$  obtained from (11). Hence,  $\check{H}^1$  can detect complex structural behavior of tilings, but calculating the full diffraction spectrum may require further analysis [25]. Another counterexample is provided by the Rudin-Shapiro tiling, which has continuous diffraction spectrum but a highly sparse pure-point energy spectrum [5, 10, 25, 39, 40].

Topology is often invoked to explain the resilience of specific properties to external perturbations, e.g. disorder. The underlying idea being that a physical quantity expressible as a topological invariant, will remain unchanged/protected against such perturbations, like the celebrated quantum Hall conductance directly related to a topological (Chern) number. It is interesting to assess this topological protection for aperiodic tilings. Topological quantities—either structural or spectral—result from  $\check{H}^1$  and depend on sets of integers as in (5) and (6) for winding numbers, Bragg peaks and spectral gaps locations. The sensitivity of these physical quantities has been tested against increasing disorder strength and indeed appeared to be surprisingly resilient [21].

## ACKNOWLEDGMENTS

This work was supported by the Israel Science Foundation Grant No. 924/09 and the Pazy Research Foundation. We thank C. Schochet for fruitful discussions.

---

\* [eric@physics.technion.ac.il](mailto:eric@physics.technion.ac.il)

- [1] M. Senechal, *Quasicrystals and Geometry* (Cambridge University Press, 1996).  
 [2] S. Mozes, *J. Anal. Math.* **53**, 139 (1989).  
 [3] D. Levine and P. J. Steinhardt, *Phys. Rev. Lett.* **53**, 2477 (1984).  
 [4] D. Shechtman, I. Blech, D. Gratias, and J. W. Cahn, *Phys. Rev. Lett.* **53**, 1951 (1984).

- [5] J. M. Luck, *Phys. Rev. B* **39**, 5834 (1989).  
 [6] D. Damanik, M. Embree, A. Gorodetski, and S. Tcheremchantsev, *Commun. Math. Phys.* **280**, 499 (2008).  
 [7] D. Tanese, E. Gurevich, F. Baboux, T. Jacqmin, A. Lemaître, E. Galopin, I. Sagnes, A. Amo, J. Bloch, and E. Akkermans, *Phys. Rev. Lett.* **112**, 146404 (2014).  
 [8] B. Sutherland, *Phys. Rev. B* **34**, 3904 (1986).  
 [9] J. Bellissard, A. Bovier, and J.-M. Ghez, *Rev. Math. Phys.* **04**, 1 (1992).  
 [10] J. Bellissard, in *From Number Theory to Physics*, Les Houches March '89, edited by M. Waldschmidt, P. Moussa, J.-M. Luck, and C. Itzykson (Springer Berlin Heidelberg, 1992) pp. 538–630.  
 [11] D. J. Thouless, M. Kohmoto, M. P. Nightingale, and M. den Nijs, *Phys. Rev. Lett.* **49**, 405 (1982).  
 [12] M. V. Berry, *Proc. R. Soc. Lond. A* **392**, 45 (1984).  
 [13] D. J. Thouless, *Phys. Rev. B* **27**, 6083 (1983).  
 [14] D. Xiao, M.-C. Chang, and Q. Niu, *Rev. Mod. Phys.* **82**, 1959 (2010).  
 [15] H. Kunz, *Phys. Rev. Lett.* **57**, 1095 (1986).  
 [16] A. Poddubny and E. Ivchenko, *Physica E* **42**, 1871 (2010).  
 [17] Y. E. Kraus, Y. Lahini, Z. Ringel, M. Verbin, and O. Zeitlinger, *Phys. Rev. Lett.* **109**, 106402 (2012).  
 [18] Y. E. Kraus and O. Zeitlinger, *Phys. Rev. Lett.* **109**, 116404 (2012).  
 [19] M. A. Bandres, M. C. Rechtsman, and M. Segev, *Phys. Rev. X* **6**, 011016 (2016).  
 [20] F. Baboux, E. Levy, A. Lemaître, C. Gómez, E. Galopin, L. L. Gratiet, I. Sagnes, A. Amo, J. Bloch, and E. Akkermans, *Phys. Rev. B* **95**, 161114 (2017).  
 [21] A. Dareaux, E. Levy, M. B. Aguilera, R. Bouganne, E. Akkermans, F. Gerbier, and J. Beugnon, *Phys. Rev. Lett.* **119**, 215304 (2017).  
 [22] I. Dana, *Phys. Rev. B* **89**, 205111 (2014).  
 [23] A. V. Poshakinskiy, A. N. Poddubny, and M. Hafezi, *Phys. Rev. A* **91**, 043830 (2015).  
 [24] K. A. Madsen, E. J. Bergholtz, and P. W. Brouwer, *Phys. Rev. B* **88**, 125118 (2013).  
 [25] E. Akkermans, Y. Don, J. Rosenberg, and C. L. Schochet, *J. Geom. Phys.* **165**, 104217 (2021).  
 [26] E. Akkermans, G. V. Dunne, and E. Levy, in *Optics of Aperiodic Structures: Fundamentals and Device Applications*, edited by L. Dal Negro (Pan Stanford Publishing, 2013) pp. 407–449.  
 [27] Y. Don and E. Akkermans, (2021), See Supplementary Material.  
 [28] E. Levy, A. Barak, A. Fisher, and E. Akkermans, Topological properties of Fibonacci quasicrystals : A scattering analysis of Chern numbers (2015), [arXiv:1509.04028](https://arxiv.org/abs/1509.04028) [physics.optics].  
 [29] E. Levy and E. Akkermans, *Eur. Phys. J. Special Topics* **226**, 1563 (2017).  
 [30] J. M. Luck, in *Fundamental Problems in Statistical Mechanics, VIII*, edited by M. H. Ernst and H. van Beijeren (Elsevier, 1994) pp. 127–167.  
 [31] M. Duneau and A. Katz, *Phys. Rev. Lett.* **54**, 2688 (1985).  
 [32] A. Katz and M. Duneau, *J. Phys. France* **47**, 181 (1986).  
 [33] A. Julien, *Ergod. Th. Dynam. Sys.* **30**, 489 (2009).  
 [34] E. Arthur Robinson, Jr., in *Symbolic dynamics and its applications*, Proceedings of Symposia in Applied Mathematics, Vol. 60, edited by S. Williams (American Mathematical Society, 2004) pp. 81–120.

- [35] Y. Don, *Topological Properties of Aperiodic Tilings and Fractals*, **PhD Thesis**, Technion – Israel Institute of Technology (2021).
- [36] R. Johnson and J. Moser, *Commun. Math. Phys.* **84**, 403 (1982).
- [37] R. A. Johnson, *J. Differ. Equ.* **61**, 54 (1986).
- [38] F. Delyon and B. Souillard, *Commun. Math. Phys.* **89**, 415 (1983).
- [39] J. M. Luck, C. Godrèche, A. Janner, and T. Janssen, *J. Phys. A* **26**, 1951 (1993).
- [40] M. Baake and U. Grimm, *Aperiodic Order*, Encyclopedia of Mathematics and its Applications, Vol. 2: Crystallography and Almost Periodicity (Cambridge University Press, 2018).
- [41] J. E. Anderson and I. F. Putnam, *Ergod. Th. Dynam. Sys.* **18**, 509 (1998).
- [42] M. Queffélec, *Substitution Dynamical Systems – Spectral Analysis*, 2nd ed., Lecture Notes in Mathematics, Vol. 1294 (Springer Berlin Heidelberg, 2010).
- [43] F. Axel and H. Terauchi, *Phys. Rev. Lett.* **66**, 2223 (1991).
- [44] Z. Cheng, R. Savit, and R. Merlin, *Phys. Rev. B* **37**, 4375 (1988).
- [45] J. Wolny, A. Wnęk, J.-L. Verger-Gaugry, and L. Pytlik, *Mater. Sci. Eng. A* **294-296**, 381 (2000).
- [46] J.-P. Gazeau and J.-L. Verger-Gaugry, *J. Théor. Nr. Bordx.* **20**, 673 (2008).
- [47] M. Kolář, B. Iochum, and L. Raymond, *J. Phys. A: Math. Gen.* **26**, 7343 (1993).
- [48] M. Baake, U. Grimm, and J. Nilsson, *Acta Phys. Pol. A* **126**, 431 (2014).

# Supplementary Material: Winding Numbers and Topology of Aperiodic Tilings

Yaroslav Don and Eric Akkermans

Department of Physics, Technion – Israel Institute of Technology, Haifa 3200003, Israel

## Appendix A: Cut and Project

In this appendix, we show how to make periodic and quasiperiodic structures using the C&P scheme.

### 1. The Procedure

The canonical C&P procedure is as follows [1].

#### Cut:

1. Start with an  $n$ -dimensional space  $R = \mathbb{R}^n$ .
2. Insert “atoms” on the integer lattice  $Z = \mathbb{Z}^n$ .
3. Divide  $R$  into the *physical space*  $E_{\parallel}$  and the *internal space*  $E_{\perp}$  such that  $E_{\parallel} \oplus E_{\perp} = R$  and  $E_{\parallel} \cap E_{\perp} = \emptyset$ .
4. To resolve ambiguity for  $E_{\parallel}$ , choose an initial location  $\mathbf{c} \in R$  such that  $E_{\parallel}$  passes through  $\mathbf{c}$ . There is no such requirement for  $E_{\perp}$ .

#### Project:

1. Inspect the hypercube  $\mathbb{I}_n = [-0.5, 0.5]^n$ .
2. The *window* is its projection on the internal space  $W = \pi_{\perp}(\mathbb{I}_n)$ .
3. The *strip* is the product with the physical space  $S = W \otimes E_{\parallel}$ .
4. Choose only the points inside the strip  $S \cap Z$ , and project them onto the physical space,  $Y = \pi_{\parallel}(S \cap Z)$ .
5. The *atomic density* is given by  $\rho(\mathbf{x}) \equiv \rho_{\mathbf{c}}(\mathbf{x}) = \sum_{\mathbf{y} \in Y} \delta(\mathbf{x} - \mathbf{y})$  with  $\mathbf{x} \in E_{\parallel}$ . Note the implicit dependency of  $Y$  on  $\mathbf{c}$ .

The C&P for  $2D \rightarrow 1D$  is given in Fig. A1. Here, there are only 2 possible distances between neighboring atoms,  $l_A, l_B$ . This gives us the notion of a *tiling* of the letters  $A$  and  $B$ . Another way to create this tiling is by moving in a stairway fashion on the atoms inside the strip: assign  $A$  to a rightwards movement and  $B$  to the upward one.

### 2. Rational Approximations by Continued Fractions

In order to work with finite systems  $w_N$ , a proper approximation method is needed for the infinite quasiperiodic system. We suggest approximating the slope  $s$  by the continued fraction

$$s = a_0 + \frac{1}{a_1 + \frac{1}{a_2 + \frac{1}{a_3 + \dots}}} = [a_0; a_1, a_2, a_3, \dots], \quad (\text{A1})$$

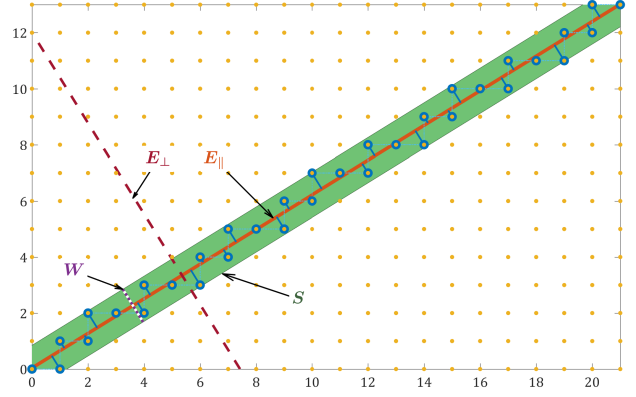


Figure A1. The cut and project scheme.

where  $a_0 \in \mathbb{Z}$  is an integer and  $a_{i \geq 1} \in \mathbb{N}$  natural numbers. Setting the approximation  $s_N = [a_0; a_1, a_2, a_3, \dots, a_N]$ , one has  $s_N \rightarrow s$  as  $N \rightarrow \infty$ . Additionally, we obtain the sequence of numerators and denominators  $s_N = c_N/d_N$ . The denominators  $d_N$  set the length of the word for the  $N$ -th approximation; the numerators  $c_N$  relate them to the phason  $\phi$  as described in the main text. We call  $w_N$  the finite approximation to  $w_{\infty}$ .

Using finite approximants of continued fractions is not only convenient but of crucial importance. The ideas of the phases presented below work only for finite structures of size  $d_N$ . So does the correspondence between all C&P models (the canonical,  $\Sigma_1$  and the characteristic function). We state that continued fractions exhibit the optimal approximation in due to the following inequality,

$$\left| s - \frac{c_N}{d_N} \right| < \frac{1}{d_N^2}. \quad (\text{A2})$$

In other words, it is the best rational approximation for any denominators smaller than  $d_N$ .

## Appendix B: Gap Labeling Theorem

In this appendix, we present succinctly how to calculate the gap labels according to the gap labeling theorem.

### 1. Gap Labeling Formula

For a  $1D$  substitution  $\sigma$  with occurrence matrix  $M$ , the possible gaps in the spectrum are given by [2]

$$\mathcal{N}_{\text{gap}} = \frac{1}{a} \frac{k}{\lambda_*^N} \pmod{1}, \quad a, k, N \in \mathbb{N}. \quad (\text{B1})$$

Here,  $\lambda_*$  is the leading (largest) eigenvalue of  $M$ . The calculation of the normalization factor  $a$  is given below. For  $d = \det(M) \neq 0$ , this can be rewritten as

$$\mathcal{N}_{\text{gap}} = \frac{1}{a} \frac{p+q/\lambda_*}{d^N} \pmod{1}, \quad p, q \in \mathbb{Z}. \quad (\text{B2})$$

For a 1D C&P tiling with slope  $s$ , the possible gaps are given by

$$\mathcal{N}_{\text{gap}} = p + qs \pmod{1}, \quad p, q \in \mathbb{Z}. \quad (\text{B3})$$

## 2. Calculation of the Normalization Factor

Let us introduce letter doublets  $L_k = l_i l_j$ , where  $l_i l_j$  are all *possible neighbors* in  $w_\infty$ . We then rewrite  $w_\infty$  in terms of  $L_k$  denoting it  $w_\infty^2$ . We denote the set of all doublets as  $\Gamma_2 = \{L_k\} = \{\alpha, \beta, \gamma, \dots\}$ .

The next step to define a substitution  $\sigma_2 : \Gamma_2 \rightarrow \Gamma_2^{\mathbb{N}}$ . It is done as follows for each letter  $L \in \Gamma_2$  [3].

- (a) Translate back to  $L = l_1 l_2 \dots l_m$  where  $l_i \in \Gamma_1$ ;
- (b) Apply  $\sigma(L) = \sigma(l_1 l_2 \dots l_m) = \ell_1 \ell_2 \dots \ell_n$ ;
- (c) Calculate the length  $d = |\sigma(l_1)|$ ;
- (d) Define  $S = \ell_1 \ell_2 \dots \ell_{d+1}$ ;
- (e) Translate  $S = L_1 \dots L_d$  in terms of  $\Gamma_2$ .

Then, the definition of  $\sigma_2$  reads

$$\sigma_2(L) = S, \quad \forall L \in \Gamma_2. \quad (\text{B4})$$

We then define the occurrence matrix  $M_2$  similarly to  $M$ . The eigenvalues of  $M_2$  contain all eigenvalues of  $M$ . Specifically, they have the same leading eigenvalue  $\lambda_*$ .

Next, calculate  $a$  as follows. Take the respective leading left-eigenvectors  $\mathbf{v}_*^L$  and  $\mathbf{v}_{*,2}^L$ . Inspect all their entries  $v_i$ . The least common multiplier of all  $v_i$  (removing factors of  $\lambda_*$ ) is  $a^{-1}$ .

For example, in the Fibonacci substitution,  $\Gamma_1 = \{A, B\}$  and  $\sigma(A) = AB$ ,  $\sigma(B) = A$ , one finds that  $\Gamma_2 = \{\alpha = AA, \beta = AB, \gamma = BA\}$ . Using the algorithm above, we obtain

$$\sigma_2^{\text{Fib}} : \begin{cases} \alpha \mapsto \beta\gamma, \\ \beta \mapsto \beta\gamma, \\ \gamma \mapsto \alpha; \end{cases} \quad (\text{B5})$$

with the occurrence matrix

$$M_2^{\text{Fib}} = \begin{pmatrix} 0 & 1 & 1 \\ 0 & 1 & 1 \\ 1 & 0 & 0 \end{pmatrix}. \quad (\text{B6})$$

Additionally,  $\lambda_*^{\text{Fib}} = (\sqrt{5} + 1)/2$  and  $a_{\text{Fib}} = 1$ .

## 3. Primitivity Condition

The primitivity of  $M$  and  $M_2$  ensures that

- (a) the leading eigenvalue  $\lambda_*$  is unique, real and positive;
- (b) the leading eigenvectors  $\mathbf{v}_*^L$  and  $\mathbf{v}_{*,2}^L$  have strictly positive entries  $v_i$  [4, 5].

These  $v_i$  are interpreted as corresponding letter  $l_i$  frequency in the infinite word  $w_\infty$  [6]. They are used as probability measures in the calculation of GLT [2]. The Perron-Frobenius theorem above also holds for a general non-strictly-upper-triangular nonnegative matrix  $M$  (see Thm. 2.20 in [4]) up to the uniqueness of  $\lambda_*$ .

## Appendix C: Čech Cohomology and $\zeta$ -function

The natural topological group associated with tilings is the Čech cohomology [7]. Its exact definition is beyond the scope of this paper (see [8] for an introduction). Nonetheless, we show in this section how to calculate the groups  $\check{H}^0$  and  $\check{H}^1$  with integer coefficients.

### 1. Bratteli Diagrams

In this section, we show how to construct the Bratteli diagrams [7, 8]. We use the Fibonacci substitution  $A \mapsto AB$ ,  $B \mapsto A$  as an illustrative example.

Consider the shift-map  $\gamma_n : \Gamma_n \rightarrow \Gamma_n$  defined by

$$\gamma_n(w_i) = w_j \quad \text{if } w_j \text{ follows } w_i \text{ in } w_\infty. \quad (\text{C1})$$

The graphical representation of  $\gamma_n$  is a Bratteli diagram  $G_n$ . Its nodes are in  $\Gamma_n$  and edges are in  $\Gamma_{n+1}$ . For Fibonacci, the first few diagrams are

$$G_0^{\text{Fib}} = A \begin{array}{c} \circlearrowleft \\ \circlearrowright \end{array} B \quad (\text{C2a})$$

$$G_1^{\text{Fib}} = AA \begin{array}{c} \circlearrowleft \\ \circlearrowright \end{array} \begin{array}{c} \xrightarrow{AB} \\ \xleftarrow{BA} \end{array} B \quad (\text{C2b})$$

$$G_2^{\text{Fib}} = \begin{array}{c} \begin{array}{c} \circlearrowleft \\ \circlearrowright \end{array} AA \begin{array}{c} \xrightarrow{BAA} \\ \xleftarrow{ABA} \end{array} \begin{array}{c} \circlearrowleft \\ \circlearrowright \end{array} BA \\ \begin{array}{c} \xrightarrow{AAB} \\ \xleftarrow{BAB} \end{array} \begin{array}{c} \circlearrowleft \\ \circlearrowright \end{array} AB \end{array} \quad (\text{C2c})$$

The zeroth diagram  $G_0^{\text{Fib}}$  indicates that  $w_\infty^{\text{Fib}}$  consists of  $A$  and  $B$  tiles.  $G_1^{\text{Fib}}$  infers that  $A$  is followed by either  $A$  or  $B$  in  $w_\infty^{\text{Fib}}$ , but  $B$  is followed by  $A$  only. This argument carries to  $G_{n \geq 2}^{\text{Fib}}$ . More diagrams are shown in Fig. C1.

Next, define the boundary operators on  $G_n$  by

$$\partial_0(\alpha) = 0, \quad \alpha, \beta \in \Gamma_n, \quad (\text{C3a})$$

$$\partial_1(e) = \beta - \alpha, \quad e = \overline{\alpha\beta} \in \Gamma_{n+1}. \quad (\text{C3b})$$



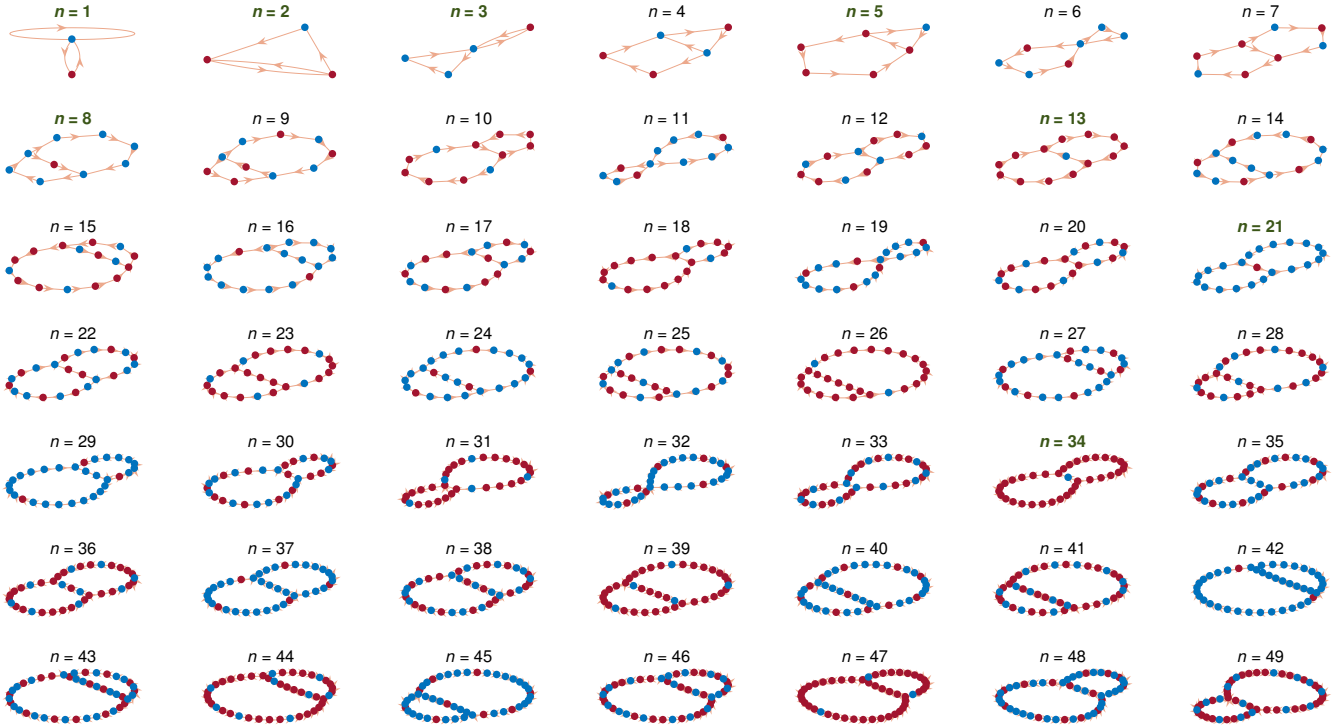


Figure C1. Bratteli diagrams for  $n = 1 \dots 49$  of the C&P Fibonacci tiling with  $s = \tau^{-2}$  and  $\tau = (\sqrt{5} + 1)/2$ . Green titles indicate  $n = d_N$ . Blue and red nodes indicate different families identified by  $L_N(n)$ , the number of  $B$ -tiles in each supertile of size  $n$  (explicitly,  $L_B^I(n) = \lfloor n \cdot s \rfloor$  for the blue nodes and  $L_B^H(n) = \lceil n \cdot s \rceil$  for the red ones). Yellow arrows indicate the edges.

The  $\partial_k$  operators are represented as matrices  $|\Gamma_n| \times |\Gamma_{n+1}|$  over  $\mathbb{Z}$ . Define the coboundary by

$$\delta^k = \partial_k^\top. \quad (\text{C4})$$

Define the simplicial cohomology of a complex  $G_n$  by

$$H_n^k = \frac{\ker \delta^k}{\text{im } \delta^{k+1}} = \frac{\text{coker } \partial_k}{\text{coim } \partial_{k+1}}, \quad (\text{C5})$$

where  $(\text{coker } d) \ker d$  is the (co)kernel of  $d$ , and  $(\text{coim } d) \text{im } d$  is its (co)image.

## 2. Čech Cohomology Calculation

The Čech cohomology is formally defined as the inverse limit of all  $H_n^k$

$$\check{H}^k = \varprojlim H_n^k. \quad (\text{C6})$$

The exact definition of this limit appears in [7, 8]. To calculate  $\check{H}^k$ , we apply  $\sigma$  on  $G_n$  as follows.

1) Apply  $\sigma_{n+1}$  on the edges of  $G_n$ .

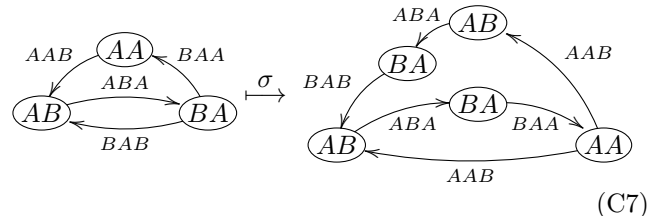
- The calculation of  $\sigma_n$  is a generalization of the procedure in Appendix B2 from  $\Gamma_2$  to  $\Gamma_n$ . Explicitly, redefine  $S = \ell_1 \ell_2 \dots \ell_{d+n-1}$  in step (d).

- A slightly different version of  $\sigma_n$  appears in [7, 8] based on “collared tiles”. For  $\sigma_3$ , denote  $e = |\sigma(\ell_2)|$  and set  $S = \ell_d \ell_{d+1} \dots \ell_{d+e+1}$  in step (d).

2) Deduce the nodes as the heads and tails of relevant edges in  $\sigma(G_n)$ .

3) Compute the inflation matrices  $A_0 : \Gamma_n \rightarrow \Gamma_n$  and  $A_1 : \Gamma_{n+1} \rightarrow \Gamma_{n+1}$  by identifying the transformation of the nodes and edges, respectively.

To calculate  $\check{H}^k$ , compute  $A_0$  and  $A_1$  of  $G_2$  (though  $G_0$  may also work in some cases). In Fibonacci,



Inspecting the nodes,  $AA \rightarrow AB$ ,  $AB \rightarrow AB$  and  $BA \rightarrow AA$  (ignoring all the extra nodes in  $\sigma(G_2)$ ). For the edges,  $\overline{AAB} \rightarrow \overline{ABA} \overline{BAB}$ , and so on. Summarizing, we arrive to  $A_0$  and  $A_1$  as follows

$$A_1^\top = \begin{pmatrix} 0 & 1 & 0 & 1 \\ 0 & 1 & 1 & 0 \\ 1 & 0 & 0 & 0 \\ 1 & 0 & 0 & 0 \end{pmatrix}, \quad A_0^\top = \begin{pmatrix} 0 & 1 & 0 \\ 0 & 1 & 0 \\ 1 & 0 & 0 \end{pmatrix}. \quad (\text{C8})$$

With the inflation matrices  $A_0$  and  $A_1$ , the  $\zeta$ -function is given by [7]

$$\zeta(z) = \frac{\det(I - zA_0^T)}{\det(I - zA_1^T)} = \frac{p_0(z)}{p_1(z)}. \quad (\text{C9})$$

The Čech cohomology can be deduced from  $p_m(z)$  by decomposing it to its irreducible components over the integers [9]. Namely, if

$$p_k(z) = \prod_{i=1}^I (1 - c_i z) \prod_{j=1}^J (1 - d_j z - e_j z^2), \quad (\text{C10})$$

with  $c_i, d_j, e_j \in \mathbb{Z}$ , then

$$\check{H}^k \cong \mathbb{Z}[c_1^{-1}] \oplus \cdots \oplus \mathbb{Z}[c_I^{-1}] \oplus \mathbb{Z}^2[e_1^{-1}] \oplus \cdots \oplus \mathbb{Z}^2[e_J^{-1}], \quad (\text{C11})$$

with  $\mathbb{Z}[1/c] = \{n/c^m \mid n, m \in \mathbb{Z}\}$ . Irreducible polynomials of higher orders are naturally generalized.

For example, in Fibonacci,

$$\zeta_{\text{Fib}}(z) = \frac{1 - z}{1 - z - z^2}. \quad (\text{C12})$$

The numerator is trivial; the denominator has 2 irrational roots. Hence,

$$\check{H}_{\text{Fib}}^0 \cong \mathbb{Z}, \quad (\text{C13a})$$

$$\check{H}_{\text{Fib}}^1 \cong \mathbb{Z}^2. \quad (\text{C13b})$$

Generally, in any tiling space,  $\check{H}^0 \cong \mathbb{Z}$  implying the tiling space is connected. Notice that if  $\deg p_1 < |\Gamma_1|$ , it implies one of the  $c_i = 0$  in  $p_1$ . Therefore, (C13) is no longer valid. These are periodic substitutions; we therefore set  $\check{H}^1 \cong \mathbb{Z}$  in this case.

The above procedure is for 1D tilings. In 2D tilings, the calculation of  $\check{H}^0$ ,  $\check{H}^1$  and also  $\check{H}^2$  is more convoluted, and  $\zeta(z)$  is not sufficient. The exact details appear in [7, 8].

### 3. Complexity

Define the *complexity* by the number of *nodes* in each complex [10]

$$c_n = |\Gamma_n|. \quad (\text{C14})$$

Now, inspect the projection maps  $\pi_n : \Gamma_{n+1} \rightarrow \Gamma_n$  between the complexes

$$\Gamma_0 \xleftarrow{\pi_0} \Gamma_1 \xleftarrow{\pi_1} \Gamma_2 \xleftarrow{\pi_2} \Gamma_3 \xleftarrow{\pi_3} \dots \quad (\text{C15})$$

which act by omitting the last letter in  $\Gamma_{n+1}$ .

There is a well-defined inverse limit [8]

$$\Omega = \varprojlim \Gamma_n. \quad (\text{C16})$$

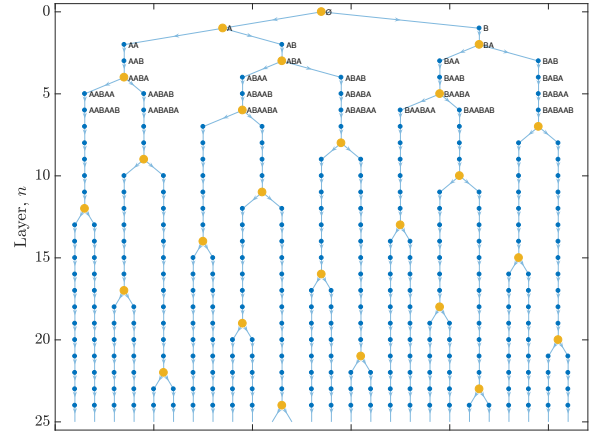


Figure C2. The complexity graph for the Fibonacci tiling. The arrows represent the mapping  $\gamma_n$ . In blue, the  $n$ -nodes ( $n$ -letter words) for each level (row)  $n$ , and in yellow – the  $n$ -nodes that split by  $\gamma_n$  into two  $(n+1)$ -nodes. The total sum of splits at each row  $n$  gives  $s_n$ . The first few nodes are labeled.

Here  $\Omega$  is the tiling space to consider. Inspect the inverse maps  $\pi_n^{-1}$ , which give the options for the last adjacent letter to create  $\Gamma_{n+1}$  from  $\Gamma_n$ . In other words,  $\pi_n^{-1}$  correspond to the *edges* in the Bratteli diagram; thus

$$\pi_n^{-1} = \gamma_n. \quad (\text{C17})$$

Hence, define the complexity tree  $T_n$  by the sequence

$$T_n = \Gamma_0 \xrightarrow{\gamma_0} \Gamma_1 \xrightarrow{\gamma_1} \Gamma_2 \xrightarrow{\gamma_2} \dots \xrightarrow{\gamma_{n-1}} \Gamma_n. \quad (\text{C18})$$

This is seen in Fig. C2.

Consider the *splits* at each level  $\Gamma_n$  as shown in Fig. C2. Here,  $y_n$  is the number of nodes in level  $n$  that have  $> 1$  *outgoing* edges, and  $s_n$  is the total number of splits. Note that for binary substitutions,  $y_n = s_n$ .

Now, since  $\beta_n^1$  counts the number of cocycles in  $\Gamma_n$  and the Bratteli graphs are connected ( $\beta_n^0 = 1$  for all  $n$ ), each split contributes an additional cocycle. Thus

$$\beta_n^1 = s_n + 1. \quad (\text{C19})$$

Next, inspect the complexity  $p(n) = c_n$ , the total number of letters at level  $n$ . At each level  $n$ ,  $s_{n-1}$  letters are added to the letters of the  $(n-1)$ -th level; thus

$$c_n = s_{n-1} + c_{n-1}, \quad c_0 = 1. \quad (\text{C20})$$

Therefore,

$$c_n = 1 + \sum_{i=0}^{n-1} s_i. \quad (\text{C21})$$

For C&P (Sturmian) sequences, where  $\beta_n^1 = 2$  (equally,  $s_n = 1$ ) for all  $n$ , one has  $c_n = n + 1$ . For primitive substitution tilings, the cohomology is bound,  $\beta_n^1 \leq C + 1$ ; thus  $c_n \leq Cn + 1 = O(n)$  [10, 11]. For a periodic tiling,  $\beta_{n>N}^1 = 1$  (equally,  $s_{n>N} = 0$ ) for some  $N \in \mathbb{Z}$ ; thus, the complexity is constant,  $c_{n>N} = C$ .

## Appendix D: Scattering Matrix Formalism

In this appendix, we present the spectral features of aperiodic structures. The avid reader is referred to [12, 13] for further details.

### 1. Transfer Matrix

We now present succinctly the main results of the transfer matrix in the wave equation. Consider a 1D system of size  $L$  of some dielectric material. Its wave equation reads

$$-\psi''(x) - k_0^2 v(x) \psi(x) = k_0^2 \psi(x). \quad (\text{D1})$$

One has waves incoming to the system from the left and right, and outgoing waves after transmission and reflection. The free part (without dielectrics) has a well-defined  $k$  vector, but the system itself need a more careful analysis. Next, consider scattering boundary conditions using  $v(x) = \epsilon(x)/\bar{\epsilon} - 1 = n^2(x) - 1$  with  $n(x)$  the refractive index [12]. We consider  $v(x)$  build in the same quasiperiodic manner as above using  $\Sigma_1$ . In other words, we have  $d_N$  slabs of refraction index  $n_{A,B}$  and width  $l_{A,B}$  so that  $n_A l_A = n_B l_B$  ordered in a quasiperiodic way.

If we consider our system built of different dielectric media (width and permittivity), neglecting internal losses in the system, the total transfer matrix from left to right is written as

$$\begin{pmatrix} \psi_R^i \\ \psi_R^o \end{pmatrix} = T_W \begin{pmatrix} \psi_L^i \\ \psi_L^o \end{pmatrix} = T_M \cdots T_2 T_1 \begin{pmatrix} \psi_L^i \\ \psi_L^o \end{pmatrix}, \quad (\text{D2})$$

and all the  $T_m$ -s are either propagation inside a slab or transfer between slabs as follows [12, 14]. For propagation one uses

$$T_A = \begin{pmatrix} \cos \delta_A & -\sin \delta_A \\ \sin \delta_A & \cos \delta_A \end{pmatrix}, \quad T_B = \begin{pmatrix} \cos \delta_B & -\sin \delta_B \\ \sin \delta_B & \cos \delta_B \end{pmatrix}, \quad (\text{D3})$$

where the optical path is given by  $\delta_A(k) = k n_A l_A$  with  $k$  the wavevector,  $n_A$  the refraction index of the slab of type  $A$  and  $l_A$  its width (similarly for  $\delta_B$ ). To simplify the calculations, one uses the same optical path  $\delta_A(k) = \delta_B(k) = \delta(k)$ , so that

$$n_A l_A = n_B l_B. \quad (\text{D4})$$

For the interface between slabs one uses

$$T_{A \rightarrow B} = \begin{pmatrix} 1 & 0 \\ 0 & n_B/n_A \end{pmatrix}, \quad T_{B \rightarrow A} = \begin{pmatrix} 1 & 0 \\ 0 & n_A/n_B \end{pmatrix}. \quad (\text{D5})$$

### 2. Scattering Matrix

Take the structure of slabs and perform a scattering experiment. The scattering  $\mathcal{S}$ -matrix is defined by

$$\begin{pmatrix} \vec{o} \\ \vec{\bar{o}} \end{pmatrix} = \begin{pmatrix} \vec{r}(k) & t(k) \\ t(k) & \vec{r}(k) \end{pmatrix} \begin{pmatrix} \vec{i} \\ \vec{\bar{i}} \end{pmatrix} = \mathcal{S} \begin{pmatrix} \vec{i} \\ \vec{\bar{i}} \end{pmatrix}, \quad (\text{D6})$$

with  $\vec{r} = r \exp(i\vartheta)$  and  $\vec{\bar{r}} = r \exp(i\bar{\vartheta})$  the rightwards and leftwards reflection coefficients and  $t$  is the transmission coefficient. There is a well-defined procedure to translate  $\mathcal{T}$  to  $\mathcal{S}$  (see [12, 15]). For  $\mathcal{T}(k) = \begin{pmatrix} M_1(k) & M_3(k) \\ M_2(k) & M_4(k) \end{pmatrix}$ , one has

$$\vec{r}(k) = \frac{(M_4 - M_1) + i(M_2 + M_3)}{(M_1 + M_4) + i(M_3 - M_2)}, \quad (\text{D7a})$$

$$\vec{\bar{r}}(k) = \frac{(M_1 - M_4) + i(M_2 + M_3)}{(M_1 + M_4) + i(M_3 - M_2)}, \quad (\text{D7b})$$

$$t(k) = \frac{2}{(M_1 + M_4) + i(M_3 - M_2)}. \quad (\text{D7c})$$

The  $\mathcal{S}$ -matrix is unitary and thus can be diagonalized to  $\mathcal{S} \mapsto \text{diag}(e^{i\gamma_1} \ e^{i\gamma_2})$  so that  $\det \mathcal{S} = e^{2i\delta(k)}$  is identified with the total phase shift

$$\begin{aligned} 2\delta(k) &= \gamma_1(k, \phi) + \gamma_2(k, \phi) \\ &= \text{Im} \log \det \mathcal{S}(k, \phi), \end{aligned} \quad (\text{D8})$$

independent of  $\phi$  with  $\text{Im}(z)$  the imaginary part of  $z$ . The Krein-Schwinger formula [12] allows to relate the change of density of states to the scattering data

$$\varrho(k) - \varrho_0(k) = \frac{1}{2\pi} \text{Im} \frac{d}{dk} \log \det \mathcal{S}(k), \quad (\text{D9})$$

where  $\varrho_0(k)$  is the free density of states (i.e. without the system). The integrated density of states is, therefore,

$$\mathcal{N}(k) - \mathcal{N}_0(k) = \delta(k) / \pi. \quad (\text{D10})$$

The chiral phase expresses the directionality of the  $\mathcal{S}$ -matrix. It is defined by [14]

$$\Theta_s(k, \phi) = \vec{\vartheta}(k, \phi) - \vec{\bar{\vartheta}}(k, \phi), \quad (\text{D11})$$

which is  $\phi$ -dependent. Inside the gaps,  $r = 1$  and  $t = 0$ ; thus, the  $\mathcal{S}$ -matrix is diagonal, and we can identify  $\gamma_1 = \vec{\vartheta}$  and  $\gamma_2 = \vec{\bar{\vartheta}}$ . Therefore,  $\Theta_s$  can be written as [9]

$$\Theta_s(k, \phi) = \text{Im} \text{Tr} [\sigma_z \log \mathcal{S}(k, \phi)], \quad (\text{D12})$$

where  $\sigma_z = \text{diag}(1 \ -1)$  is the Pauli matrix.

- 
- [1] M. Duneau and A. Katz, *Phys. Rev. Lett.* **54**, 2688 (1985).
  - [2] J. Bellissard, A. Bovier, and J.-M. Ghez, *Rev. Math. Phys.* **04**, 1 (1992).
  - [3] M. Queffelec, *Substitution Dynamical Systems - Spectral Analysis*, 2nd ed., Lecture Notes in Mathematics, Vol. 1294 (Springer Berlin Heidelberg, 2010).
  - [4] R. S. Varga, *Matrix Iterative Analysis*, 2nd ed. (Springer Berlin Heidelberg, 2000).
  - [5] E. Seneta, *Non-negative Matrices and Markov Chains*, Rev. Print. ed., Springer series in statistics (Springer New York, 2006).

- [6] J. M. Luck, C. Godrèche, A. Janner, and T. Janssen, *J. Phys. A* **26**, 1951 (1993).
- [7] J. E. Anderson and I. F. Putnam, *Ergod. Th. Dynam. Sys.* **18**, 509 (1998).
- [8] L. A. Sadun, *Topology of Tiling Spaces*, University Lecture Series, Vol. 46 (American Mathematical Society, 2008).
- [9] Y. Don, *Topological Properties of Aperiodic Tilings and Fractals*, *PhD Thesis*, Technion – Israel Institute of Technology (2021).
- [10] A. Julien, *Ergod. Th. Dynam. Sys.* **30**, 489 (2009).
- [11] E. Arthur Robinson, Jr., in *Symbolic dynamics and its applications*, Proceedings of Symposia in Applied Mathematics, Vol. 60, edited by S. Williams (American Mathematical Society, 2004) pp. 81–120.
- [12] E. Akkermans, G. V. Dunne, and E. Levy, in *Optics of Aperiodic Structures: Fundamentals and Device Applications*, edited by L. Dal Negro (Pan Stanford Publishing, 2013) pp. 407–449.
- [13] E. Akkermans and G. Montambaux, *Mesoscopic Physics of Electrons and Photons* (Cambridge University Press, 2011).
- [14] E. Levy, *Topological properties of quasiperiodic chains: structural and spectral analysis*, *PhD Thesis*, Technion – Israel Institute of Technology (2016).
- [15] E. Levy and E. Akkermans, *Eur. Phys. J. Special Topics* **226**, 1563 (2017).